Optical properties of ocular tissues in the near infrared region

Dhiraj K. Sardar[1], Raylon M. Yow[1], Guang-Yin Swanland[1], Robert J. Thomas[2], and Andrew T. C. Tsin[3]

[1]Department of Physics and Astronomy, The University of Texas at San Antonio, San Antonio, Texas 78249-0697
[2]Air Force Research Laboratory, Brooks City-Base, Texas 78235-5128
[3] Department of Biology, The University of Texas at San Antonio, San Antonio, Texas 78249-0662

ABSTRACT

Near infrared characterization of optical properties of various tissue components of healthy human and bovine eyes has been performed. The indices of refraction (n) of these ocular tissues were determined using a Michelson interferometer. The total diffuse reflection (R_d) and total transmission (T_t) measurements have been taken for individual ocular tissue by using double-integrating spheres and infrared laser diodes. The Inverse Adding Doubling computational method based on the diffusion approximation and radiative transport theory is applied to the measured values of n, R_d, and T_t to calculate the optical absorption and scattering coefficients of the human and bovine ocular tissues. The scattering anisotropy value was determined by iteratively running the inverse adding doubling method program and a Monte Carlo simulation of light-tissue interaction until the minimum difference in experimental and computed values for R_d and T_t were realized. A comparison between the optical characterization of human and bovine ocular samples is also made.

Keywords: Human Ocular Tissues, Bovine Ocular Tissues, Optical Properties, Infrared Diode Lasers

1 INTRODUCTION

Almost immediately after the advent of the first laser in 1960, the medical applications of optical radiation, especially for diagnosis and treatment of ocular diseases had begun. The use of various lasers has steadily increased over the past several years. The fundamental optical properties of tissues influence the distribution and propagation of photons in laser-irradiated tissues. Therefore, understanding the fundamental optical properties of tissues has become imperative. There had been some studies in the past on ocular tissues.[1-9] However, to the best of our knowledge, a systematic investigative comparison of the optical properties of human and bovine ocular tissue components has not been performed, particularly, in the near infrared region (1.2 - 1.4 μm) where the eye transitions from strongly transmissive to strongly absorbing.[7] Construction of diagnostic or imaging devices for ocular diseases in the spectral range of interest will require a detailed knowledge of optical parameters to predict performance and effectiveness. Also, the prediction of safe exposure limits requires a quantitative knowledge of these parameters for predicting damage thresholds to various components of the eye.[10-12] In this article, we therefore present a characterization and comparison of the refractive indices, optical absorption and scattering properties of cornea, crystalline lens, vitreous humor, and aqueous humor from a healthy human eye and healthy bovine eye.

Due to the complex nature of the biological tissues, both the absorption and scattering properties of ocular tissues must be understood thoroughly for laser dosimetry and medical applications of lasers. The quantitative distribution of light intensity in biological media can be obtained from the solution of the Chandrasekhar's radiative transport equation: [13]

$$\frac{dI(\mathbf{r},\mathbf{s})}{ds} = -(\mu_a+\mu_s) I(\mathbf{r},\mathbf{s}) + \frac{\mu_a+\mu_s}{4\pi}\int_{4\pi} p(\mathbf{s},\mathbf{s}') I(\mathbf{r},\mathbf{s}')\, d\Omega', \quad (1)$$

where $I(\mathbf{r},\mathbf{s})$ is the intensity per unit solid angle at the target location $\mathbf{r}$ in the direction $\mathbf{s}$ ($\mathbf{s}$ is the directional unit vector),

Ophthalmic Technologies XVI, edited by Fabrice Manns, Per G. Söderberg, Arthur Ho,
Proc. of SPIE Vol. 6138, 613815, (2006) · 1605-7422/06/$15 · doi: 10.1117/12.643874

μ_a and μ_s are the absorption coefficient and scattering coefficient, respectively, p(s,s') is the phase function, representing scattering contribution from the direction s' to s, and Ω' is the solid angle. The first term on the right hand side of Eq. (1) represents the loss in intensity per unit length in direction s due to absorption and scattering, while the second term denotes the gain per unit length due to scattering from direction s'.

An analytical solution to Eq. (1) has been difficult to achieve due to the complex nature of biological media and their inherent inhomogeneities and irregularities in the physical shape. However, an approximate solution can be obtained by assuming homogeneity and regular geometry of the medium. Although the functional form of the phase function in biological media is generally unknown for many practical applications, the Henyey-Greenstein formula, Eq. (2), provides a good approximation of the phase function for turbid media: [14]

$$p(\theta) = \frac{1}{4\pi} \frac{1 - g^2}{\left(1 + g^2 - 2g\cos\theta\right)^{3/2}}, \tag{2}$$

where θ is the angle between s and s'. The Henyey-Greenstein phase function depends only on the scattering anisotropy coefficient g, which is defined as the mean cosine of the scattering angle and expressed as follows:

$$g = \frac{\int_{4\pi} p(v)\, v\, d\Omega'}{\int_{4\pi} p(v)\, d\Omega'}. \tag{3}$$

The value of g ranges from −1 for complete backward scattering to +1 for the complete forward scattering. The anisotropy value of zero corresponds to isotropic scattering.

Recently, Prahl et al. have introduced an important numerical approach known as the Inverse Adding Doubling (IAD) method[14] to solve the transport equation, Eq. (1). The IAD method[14] in conjunction with the Monte Carlo (MC) simulation technique[15-17] is currently being used to obtain a more accurate estimate of optical properties of turbid media such as biological samples. Details of the IAD method have been previously provided by Prahl et al.[14] Nonetheless, to maintain a continuity in this article, a short synopsis of the IAD model is provided here. Two dimensionless quantities used in the entire IAD method are albedo (a) and optical depth (τ), which are defined as follows:

$$a = \mu_s / (\mu_s + \mu_a) \tag{4}$$

and

$$\tau = t(\mu_s + \mu_a), \tag{5}$$

where t is the physical thickness of the sample measured in cm. Values of n, g, R_d, and T_t are input to the IAD computer program which returns the values of a and τ. Values of these dimensionless quantities are then applied to Eqs. (4) and (5) to solve for μ_s and μ_a of the human and bovine ocular tissues. Further details of the IAD method can be found in Ref. (14). According to Prahl et al.,[14] the validity of the IAD method for samples with comparable absorption and scattering coefficients is especially important, since other methods based on only diffusion approximation are inadequate.[18] They have also stated that since both anisotropy phase function and Fresnel reflection at boundaries is accurately approximated, the IAD method is well suited to optical measurements for biological materials sandwiched between two glass slides.

Values of the absorption, scattering, and scattering anisotropy coefficients are needed for the approximate solution to the transport equation. Therefore, appropriate experimental methods are necessary to measure n, R_d, and T_t that in turn produce the values of absorption, scattering, and scattering anisotropy coefficients. In this article, we present an in-depth characterization of optical properties of human and bovine ocular tissues at 980, 1310, and 1530 nm.

2 MATERIALS AND METHODS

2.1 Tissue Samples Preparation

One pair of healthy human eyes was obtained from the National Drug Research Interchange (NDRI) within 24 hours of harvesting. These eyes were shipped on ice to preserve their physiological and optical properties. Immediately upon arrival of the eyes at the biological laboratory, they were carefully dissected. The individual components including cornea, lens, aqueous humor, and vitreous humor were removed and placed in between glass slides. The prepared tissue samples were then placed on ice and transported to the laser laboratory where optical measurements were immediately performed.

In addition, a pair of healthy bovine eyes was obtained from a local slaughterhouse immediately after being removed from the animal. The handling of the bovine eyes was identical to that of the human eyes described above.

2.1.1 Aqueous Humor and Vitreous Humor Sample Preparation

Reservoirs to hold the aqueous humor and vitreous humor for optical measurements were constructed from 1-mm-thick glass slides and epoxy. The aqueous humor was carefully removed from the eye using a 1.0 cc needle syringe and injected into one of the reservoirs. The same procedure was used for the vitreous humor sample.

2.1.2 Crystalline Lens Tissue Preparation

After extraction of the vitreous humor, the lens could easily be removed from the eye cup. Because of its small size, the human lens was kept intact and placed on a glass slide. For the bovine lens, a razor blade was used to remove a slice from the front of the lens which was placed on a glass slide. For both samples, the lens tissue was surrounded with modeling clay and a second glass slide was placed on top and minimal pressure was applied to remove any gap between the lens and glass slides. It is important to mention that when pressure was applied to the lens tissue, extra precaution was taken so that the optical properties of the tissue remained intact.

2.1.3 Cornea Tissue Preparation

Since the cornea is stretched around the eye cup, it tends to shrink and wrinkle after being removed from the eye cup. It was therefore mounted on a clean glass slide immediately after it is was separated from the eye cup to obtain a flat sample. The method for mounting the cornea sample was the same as that of the lens.

2.1.4 Sample Thickness

Thicknesses of all tissue samples were measured using a digital caliper. The thickness of the human aqueous humor sample was measured to be approximately 1.02 mm, the human vitreous humor sample was approximately 2.02 mm, the human lens tissue was approximately 2.75 mm, and the human cornea tissue was approximately 2.46 mm. The thickness of the bovine aqueous humor sample was measured to be approximately 1.02 mm, the bovine vitreous humor sample was approximately 2.01 mm, the bovine lens tissue was approximately 1.50 mm, and the bovine cornea tissue was approximately 1.21 mm. All measurements of thickness were taken from the total thickness of the sample holder minus 2 mm for the thickness of two glass slides.

2.2 Measurement of Diffuse Reflectance and Transmittance

The total diffuse reflectance and total transmittance were measured using two identical integrating spheres (Oriel model 70451). The tissue sample was placed in a specially designed holder that coupled the two integrating spheres. The measurements were performed on the aqueous humor, vitreous humor, cornea, and crystalline lens of the human eye at 980, 1310, and 1530 nm. The 980 and 1310 nm wavelengths were from pig-tailed diode lasers (Thorlabs model L9805E2P5 and Mitsubishi ML725B8F, respectively) coupled to collimators (Thorlabs model F220FC-C) and controlled by a Thorlabs (model LDC 2000) laser driver. The laser beam diameter at $1/e^2$ of the peak intensity was 1.97 mm and beam divergence was about 0.048°. The 1530 nm wavelength was supplied by a pig-tailed erbium fiber

amplified stimulated emission module (NP Photonics model ASE SMP-4010) coupled to a collimator (Thorlabs model F220FC-1550) and controlled by NP Photonics supplied software. The laser beam diameter at $1/e^2$ of the peak intensity was 2.07 mm and beam divergence was about 0.055°. The average output power was kept at about 0.25 mW for all optical measurements.

The schematic of the experimental setup for measuring the total diffuse reflectance and total transmittance is shown in Fig.1. The laser beam was directed into the entrance port A of integrating sphere 1, whose exit port is coupled with the entrance port of integrating sphere 2; the sample was mounted at the coupling port C situated in between the two integrating spheres. The exit port B of integrating sphere 2 was covered with a cap with a reflective surface identical to that of the integrating spheres. The diameter of each sphere was 6 inches and each port had a diameter of 1 inch. Light leaving the sample reflected multiple times from the inner surfaces of the spheres before reaching the detectors. Baffles within the spheres shielded the detectors from receiving the direct reflected and transmitted light from the sample. The reflected and transmitted light intensities were detected by two identical infrared detectors (Judson model J16-D); these were attached to the two measuring ports of the integrating spheres 1 and 2. The detector signal was sent to identical preamplifiers (Judson model PA-9) powered by a common power supply (Pasco model 8000). Signals from the detectors were measured by a digital oscilloscope (Tektronix model TDS3054B). The measured light intensities were then utilized to determine the total diffuse reflectance R_d and total transmittance T_t by the following expressions:

$$R_d = \frac{X_r - C_r}{Z_r - C_r} \qquad (6) \qquad \text{and} \qquad T_t = \frac{X_t - C_t}{Z_t - C_t} \qquad (7)$$

where X_r is the reflected light intensity detected by Det.1 with the sample at C, Z_r is the incident intensity detected by Det.1 with no sample at C and a reflective surface at the exit port of integrating sphere 1, X_t is the transmitted light intensity detected by Det.2 with the sample at C and a reflective surface at B, and Z_t is the incident light intensity detected by Det.2 with no sample at C and with a reflective surface at B. C_r is the correction factor for the stray light measured by Det.1 with no sample at C and the exit port of sphere 1 uncovered and sphere 2 removed. C_t is the correction for Det.2 measured with no sample or light entering the sphere 2. That is C_r is the correction for light diffusion as it enters the experimental setup and C_t is the dark current correction for Det.2. There is no need to measure dark current for Det.1 since it would factor out in Eq. (6).

2.3 Inverse Adding Doubling (IAD) Method

In order to solve the radiative transport equation, the IAD computer program [14] must be supplied with the experimental values of total diffuse reflectance (R_d) and total transmittance (T_t) along with values of index of refraction (n) and scattering anisotropy (g) of the sample. The IAD program guesses a set of optical properties (a and τ) and then calculates values for R_d and T_t. This process is repeated until the calculated and measured values of R_d and T_t are within a specified tolerance. Values of a and τ provided by the IAD method are used to calculate the absorption coefficient (μ_a) and scattering coefficient (μ_s) for individual tissue using Eqs. (4) and (5).

2.4 Monte Carlo (MC) Simulation

Measurements of the total diffuse reflectance (R_d) and total transmittance (T_t) used in the IAD method to determine the optical absorption coefficient (μ_a) and scattering coefficient (μ_s) are modeled by the MC simulation technique, which uses a stochastic simulation of light interaction with biological media.[15-17] The values of μ_a and μ_s determined by the IAD method, along with the values of n, sample thickness (t), and g are input into the MC simulation model which in turn determines R_d and T_t.

3 RESULTS AND DISCUSSION

The refraction indices (n) of the human aqueous humor and human vitreous humor samples were measured with a Michelson-type interferometer at 590, 654, and 947 nm (462 and 560 nm LED's were not on hand at the time of the measurement). The measured n values varied from 1.337 to 1.357 and are given in Table 1. The indices of refraction (n) of the bovine aqueous humor and bovine vitreous humor samples were measured with the same Michelson-type interferometer at 462, 560, 590, 654, and 947 nm. The measured n values varied from 1.343 to 1.366 and are also given in Table 1. The refractive index of the bovine aqueous humor and vitreous humor were identical to within three decimal places at all wavelengths measured. Measured refractive indices for human and bovine aqueous humor and vitreous humor are shown in Fig. 2 along with the best fit to the Sellmeier's dispersion equation. The refractive indices of bovine samples fall in between the n values for the human samples. An attempt was made to measure the refractive index of the lens and cornea, but the distortion to the wavefront by the sample made this difficult. Hence, the indices of refraction of the lens and cornea in the near infrared region were approximated by subtracting 0.01 from the values reported at 590 nm in Ref. 19, which are in good agreement with dispersion relationships in Ref. 20. The value 0.01 was selected by observing the trend in the dispersion curves for the aqueous humor and vitreous humor in Fig. 2.

The average scattering anisotropy coefficient of the tissues was determined by iteratively running IAD and MC methods until the best agreement was attained between the measured and computed values of the total diffuse reflectance (R_d) and total transmittance (T_t). The anisotropy values for the human samples varied from 0.71 to 0.99 and are given in Table 2. The anisotropy values for the bovine samples varied from 0.70 to 0.99 and are given in Table 3.

The total diffuse reflectance (R_d) and total transmittance (T_t) were measured on human and bovine ocular tissue samples at 980, 1310, and 1530 nm from diode lasers. Values of R_d and T_t are for human and bovine ocular tissue samples are given in Tables 2 and 3, respectively. These values, along with the index of refraction and estimated values of the scattering anisotropy coefficient, were input into the IAD program. The output of the IAD program were the dimensionless quantities a and τ defined by Eqs. (4) and (5), respectively. The absorption and scattering coefficients were then calculated from the values of a and τ and the thickness t of the sample. The absorption coefficient (μ_a), scattering coefficient (μ_s), total attenuation coefficient ($\mu_t = \mu_a + \mu_s$), penetration depth ($1/\mu_t$), albedo (a), and optical depth (τ) for the human and bovine ocular tissues are given in Tables 2 and 3, respectively. The experimental values of total diffuse reflectance (R_d) and total transmittance (T_t) used to obtain absorption coefficient (μ_a) and scattering coefficient (μ_s) from the IAD have been compared with those generated by the MC simulation technique. These values are given in Tables 4 and 5, for the human and bovine tissue samples, respectively, at three wavelengths. Differences in R_d and T_t determined by experimental and MC techniques can be considered reasonable considering the experimental uncertainties in the measurements, as well as the complex nature of tissue samples. Tables 4 and 5 show that the absorption and scattering coefficients for the bovine ocular tissues have the same order of magnitude as those for human ocular tissues, except for μ_s for vitreous humor at 1530 nm. It is worth noting that the values of μ_a and μ_s for bovine ocular tissues closely match with those of human ocular tissues at 1310 nm. The largest discrepancy in bovine and human data is observed to occur at 1530 nm, where the absorption coefficient for the human vitreous aqueous humor (11.60 cm^{-1}) is about twice that of bovine vitreous humor (5.93 cm^{-1}). Also at 1530 nm, the scattering coefficient for the human aqueous humor and lens is about three times that of bovine. The scattering coefficient for the human vitreous humor is about 20 times that of bovine at 1530 nm. These discrepancies can be attributed to the inherent physiological differences between the bovine and human ocular tissues.

In conclusion, the values of the absorption and scattering coefficients for ocular samples reported in this study could have significant importance for modeling light transport in the eye to predict ocular damage during exposure to laser light.

ACKNOWLEDGMENTS

This work was supported in part by the Air Force Research Laboratory Human Effectiveness Directorate HBCU/MI grant FA8650-04-1-16533, Wright-Patterson Air Force Base, Dayton, Ohio, and the NSF sponsored Center for Biophotonics Science and Technology (CBST) at UC Davis under Cooperative Agreement No. PHY 0120999.

REFERENCES

1 M. Hammer, A. Roggan, D. Schweitzer, and G. Muller, "Optical properties of ocular fundus tissues – an in vitro study using the double-integrating-sphere technique and inverse Monte Carlo simulation," *Phys. Med. Biol.* **40**, 963-978 (1995).

2 T.J. van den Berg and H. Spekreijse, "Near infrared light absorption in the human eye media," *Vision Res.* **37**, 249-253 (1997).

3 E.A. Boettner and J.R. Wolter, "Transmission of the ocular media," *Invest. Ophthalmol.*, **1**, 777-783 (1962).

4 F.C. Delori and K.P. Pflibsen, "Spectral reflectance of the human ocular fundus," *Appl. Opt.* **28** (6), 1061-1077 (1989).

5 R.W. Knighton, S.G. Jacobson, and C.M. Kemp, "The spectral reflectance of the nerve fiber layer of the macaque retina," *Invest. Ophthalmol. & Visual Sci.*, **30** (11), 2393-2402 (1989).

6 J. J. Vos, A.A. Munnik, and J. Boogaard, "Absolute spectral reflectance of the fundus oculi," *J. Opt. Soc. Am.*, **55**, 573-574 (1965).

7 E. F. Maher, SAM-TR-78-32 "Transmission and absorption coefficients for ocular media of the rhesus monkey," Brooks AFB, TX, USAF School of Aerospace Medicine (1978).

8 D.K. Sardar, F.S. Salinas, J.J. Perez, and A.T.C. Tsin, "Optical characterization of bovine retinal tissues," *J. Biomed. Opt.* **9**, 624-631 (2004).

9 V.P. Gabel, R. Birngruber, et al., "Visible and near infrared absorption in pigment epithelium and choroids," XXIII Consilium Ophthalmologicum, Amsterdam, *Experta Medica* (1978).

10 A.J. Welch and G.D. Polhamus, "Measurement and prediction of thermal injury in the retina of the rhesus monkey," *IEEE Transactions in Biomedical Engineering* **MVE-31** (10): 633 (1984).

11 A.J. Welch and M. Van Gemert, *Thermal Response of Tissue to Optical Radiation*, Plenum Press, New York (1995).

12 A.N. Takata, L. Goldfinch, et al., IITRI J-TR-74-6324 "Thermal Model of Laser-Induced Eye Damage," Brooks AFB, TX, USAF School of Aerospace Medicine: 1-N35 (1984).

13 S. Chandrasekhar, *Radiative Transfer*, Dover, New York (1960).

14 S.A. Prahl, M.J. C. Van Gemert, and A. J. Welch, "Determining the optical properties of turbid media by using the inverse adding-doubling method," *Appl. Opt.* **32**, 559-568 (1993).

15 S.L. Jacques and L. Wang, "Monte Carlo modeling of light transport in tissues," *Optical-Thermal Response of Laser-Irradiated Tissue*, eds. A.J. Welch, M.J.C. van Gemert, Plenum, New York and London (1995).

16 S.A. Prahl, M. Keijzer, S.L. Jacques, and A. J. Welch, "A Monte Carlo Model of Light Propagation in Tissue," *SPIE Institute Series* **IS 5**, 102-111 (1989).

17 J. Hourdakis and A. Perris, "A Monte Carlo estimation of tissue optical properties for use in laser dosimetry," *Phys. Med. Biol.* **40**, 351-364 (1995).

18 G. Yoon, A.J. Welch, et al., "Development and Application of Three-Dimensional Light Distribution Model for Laser Irradiated Tissue," *IEEE Journal of Quantum Electronics*, **QE-23** (10): 1721-1733 (1987).
19 http://hypertextbook.com/physics/waves/refraction/
20 D.X. Hammer, A.J. Welch, et al., "Spectrally resolved white-light interferometry for measurement of ocular dispersion," *Journal of the Optical Society of America A* **16**(9): 2092-2102 (1999).

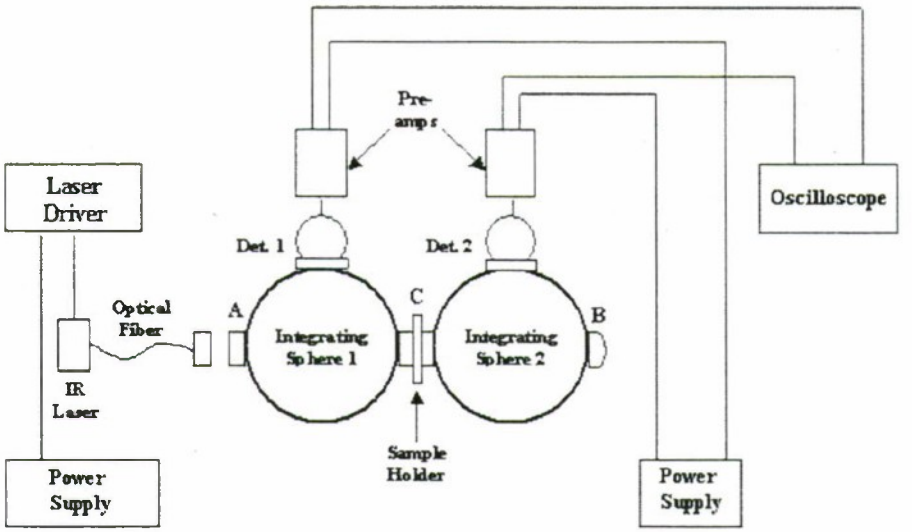

Fig. 1 Experimental schematic for the measurement of total diffuse reflectance (R_d) and total transmittance (T_t).

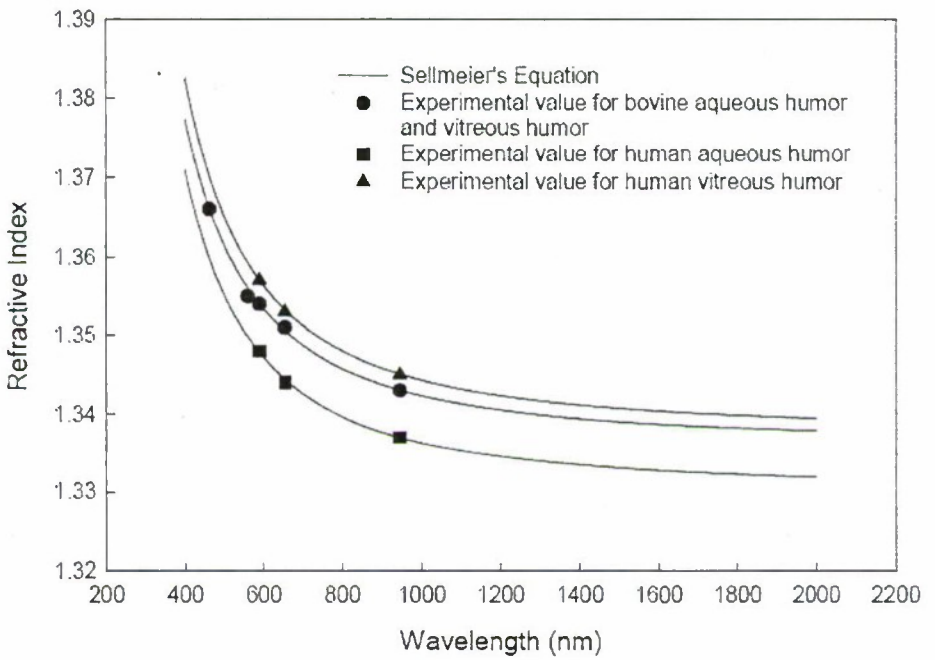

Fig. 2 Measured refractive index vs. wavelength and dispersion curves representing the best fit to Sellmeier's equation for aqueous humor and vitreous humor.